

Palm Print Recognition using Deep Learning

Ruaa Sadoon Salman, Mauj Haider AbdAlkreem*, Qaswaa Khaled Abood

Abstract: In recent decades, numerous studies have focused extensively on biometric palmprint recognition. Palm print recognition has gained significant popularity and importance across various domains owing to its exceptional efficiency and accuracy in personal identification. The biometric characterization of a person's palm print is unique. However, a way to enhance the image is needed in order to produce a better and clearer image. Recently, palm print recognition methods based on features acquired using a series of convolutional neural networks have been introduced, among which DenseNet-121 has a densely connected structure, unlike other structures. This paper presents a scheme for palm print recognition by image enhancement. Contrast-limited adaptive histogram equation (CLAHE) is one of the image enhancement methods that can provide bounded segment and region size and is based on deep learning using DenseNet-121. To measure performance, the CASIA dataset was used. Experimental results on the DS show that the palm print features of Denes 21 achieve a recognition accuracy of 99 %, demonstrating the effectiveness and reliability of the proposed palm print.

Keywords: biometric; CLAHE; deep learning; DenseNet-121; ROI

1 INTRODUCTION

Biometrics is a system that uses distinct behavioral patterns to automatically verify the identity of individuals. Physiological traits are genetic characteristics acquired during the embryonic stages of human development. The emergence of print-based biometric technology provides a promising alternative to traditional identification methods such as fingerprints, iris scanning, and facial recognition. Print recognition method datasets can be obtained easily and inexpensively due to their global and dynamic nature [1]. Biometric systems that use the palm of the hand have become of interest to researchers because they are systems with individual features that cannot be replicated among humans [2]. The importance of personal identification technology has increased in recent years, especially in authentication methods, which has led to increased research in this specialty [3, 4]. Traditional security technologies, such as passwords and magnetic cards, are no longer considered secure enough due to their susceptibility to being stolen or forgotten by the owner. Hence, in order to achieve a high level of security in interactions, biometric technologies have been developed for application in different system categories such as smart device logins, home security systems, and other control systems [5]. A palm print is a distinct biological pattern that is unique to each individual, as no two prints are identical, even among identical twins. The global use of this pattern for identification purposes is due to the fact that palm prints are not affected by external factors during the capture of the fingerprint and are similar to vein fingerprints in terms of the accuracy of the results, but the only factor that affects is the cutting of the hand or the burning of the hand and the disappearance of all lines [6, 7]. Palm or hand recognition is a key element of the biometric approach, which is widely recognized as one of the most efficient and successful means of identifying individuals. Basically, it refers to physical characteristics or behavioural traits that can be used to identify an individual [8, 9]. Palmprint-based personal authentication systems have been developed to exploit the distinctive lines, wrinkles, and features in the palm. These

characteristics create a distinct and stable pattern that remains unchanged throughout a person's lifespan [10, 11]. These systems use a camera or scanner along with its software to examine the acquired images and compare them to existing data sets in the system. It is worth noting that palm prints are equivalent to fingerprints [12]. The palm recognition system will use several techniques, including thermal methods, optical methods, and other methods, to enhance palm edges and other distinctive features [13, 14]. The goal of this research paper is to confirm the identities or recognition of individuals by analysing their Palmprint by relying on deep learning through a pre-trained model and preliminary image processing operations.

1.1 Palm Print Recognition

Print recognition employs an infrared light source to detect the presence of hemoglobin in the blood. Deoxygenated hemoglobin manifests as a dark pattern when observed with the hand or finger. The equipment thereafter records an image of the distinct patterns formed by the ridges and lines on the wrist, palm, back of the hand, finger, or face. This is analogous to the methodology employed for capturing retinal patterns [15]. According to the observation, the vascular patterns on the backs of hands and palms are more intricate compared to those on fingers. This makes them more suitable for recognition matching and authentication purposes. Similar to other methods of biometric identification, print recognition is seen as being unaffected by the passage of time and distinct enough to accurately identify an individual [16, 17]. It has been discovered that the physiological biometric can be easily counterfeited by medical procedures, leading to the loss of the person's medical identity. Therefore, it is possible to analyze and implement a powerful and resilient biometric characteristic like palm print for the purpose of identifying individuals. The presence of vitality can be determined by observing the variations in blood flow inside the print while the heart beats [18]. Fig. 1 displays the distinct regions and their corresponding labeling on the palm [6].

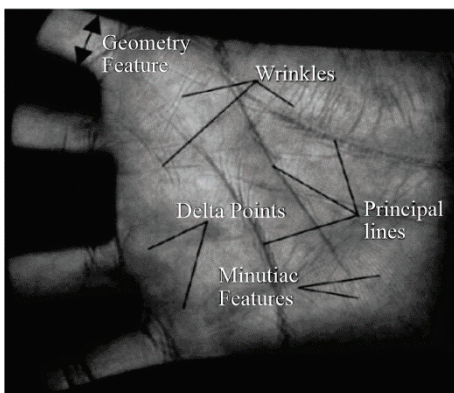


Figure 1 Principle lines, palm creases, and additional characteristics [6]

Palmprint recognition offers numerous benefits when implemented on consumer devices:

- Palmprints have comparable characteristics to fingerprints, however encompassing a far greater area.

As a result of this reasoning, they are often considered to be more durable than fingerprints [19].

- Palmprints exhibit more resistance to spoofing in comparison to faces, which are readily accessible, or fingerprints, which can be inadvertently deposited on diverse flat surfaces.
- There are no additional costs required to acquire the gadget, as long as it comes with a camera (optical sensor) and a flash output (LED or screen) [20].
- The system is capable of performing multi-biometric recognition by integrating with other hand-based features, such as fingerprints [21], finger knuckles [22], wrist [23].
- It may be easily incorporated into the functionality of various consumer gadgets, such as AR/VR headsets [20], smartphones [24], gesture control systems, driver monitoring systems, etc.

Table 1 Summarized of previous studies

Year & Ref.	Data set	Employed method	Aim of paper	Limitation	Result of System
2021 [30]	CASIA	Gabor filters block-wise histograms triple-type feature descriptor	Extracting three types of palmprint features without the need for any raining samples.	Investigate other handcrafted traits to enhance the accuracy of fingerprint recognition.	Accuracy = 88.55 %
2022 [31]	CASIA	Convolutional Neural Network VGG16	VGG16 was chosen as the central network because it replaces large kernel filters (11 and 5 in the first and second convolutional layers, respectively) with many 3x3 filters. The images are then fed into layers of convolution and max pooling until features are extracted and then classified using the SoftMax function.	Parameters. Due of its profoundness and the abundance of fully integrated layers. The model has a substantial size of 500 MB.	Accuracy = 97.32 % EER = 0.0268
2022 [32]	CASIA	Return of Investment (ROI) - Mean Robust Extended Local Binary Pattern (MRELBP) k - nearest neighbor classifier	A method for identity verification and image normalization is presented. Features are extracted in the ROI extraction step from the input photomicrograph and then reduced through dimensionality reduction and classified using a nearest neighbor classifier	This research faces some drawbacks and challenges, such as computational complexity of classification, slow speed, memory and storage issues for large data sets, and sensitivity to the choice of k and distance measure.	Accuracy = 96.6 %
2023 [33]	CASIA	Convolution Neural Network Siamese Neural Net (SNN)	An approach to handprint identification that utilizes a Siamese network. The suggested methodology involves utilizing two convolutional neural networks with shared weights to extract characteristics from handprint images. These extracted features are subsequently compared using a contrast loss function to ascertain whether the two photos originate from the same individual. Consequently performance of the Siamese can also be explored , the extracted features become more distinct and conspicuous	Feature space. The original person's template can be securely preserved in a third-party authentication system, whether trusted or untrusted, to prevent theft. It requires longer training time than regular networks, because Siamese networks include quadratic pairs to learn from. They are slower than other types. In addition, it does not extract all probabilities because the training is binary learning, so it will not produce prediction probabilities. The possibility of combining it with other deep learning techniques to improve the	Accuracy = 95.6% ERR = 0.044
2023 [34]	CASIA	Hetero-Associative Memory Encoder (HAMTE) neural network	The suggested network ensures the protection of the individual's Palmprint template by converting it into an irreversible template in a distinct	This type of memory network is commonly used in applications such as data compression and data retrieval to produce higher results and better identify people.	Accuracy = 90.2 % ERR = 0.02

2 LITERATURE REVIEW

Several studies in the literature have employed artificial intelligence (AI) to identify individuals through the utilization of Palm Print methods. The majority of palm print identification research in existing literature has employed either one or two variations of printed biometric photographs of the palm, back, or wrist. These images are often taken

using infrared or near-infrared cameras [25, 26]. For instance, the utilization of innate patterns seen in palm prints has been suggested. The camera and near-infrared illumination system of a charge-coupled device (CCD) were used to take images. Subsequently, diode and thinning techniques were employed to extract the feature, resulting in the identification of connected palm print lines and details [27, 28]. A variety of feature extraction techniques have been

employed, spanning from manual approaches to deep learning (DL) [29].

This section aims to emphasize recent advancements in biometric recognition systems utilizing multispectral imaging technology. Specifically, it will focus on the evaluation of works conducted using the CASIA database. Tab. 1 summarized the related work that mention above.

3 PROPOSED SYSTEM

The proposed system for recognition palm print is based on the pre-training model of deep learning and preprocessing images using the global stander dataset. Fig. 2 illustrates the sequential stages of the implemented system.

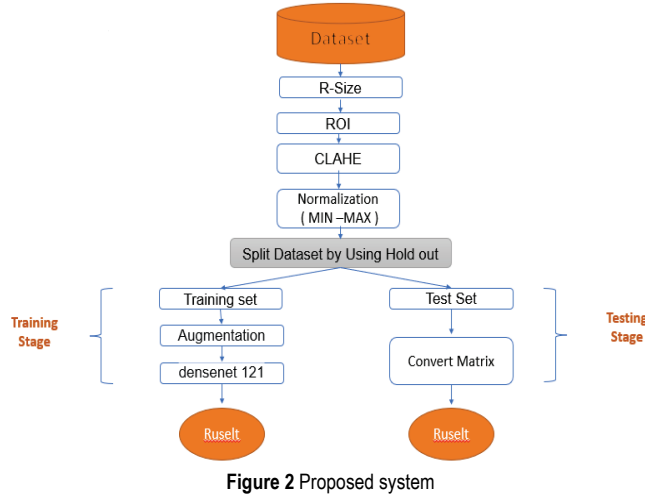


Figure 2 Proposed system

3.1 Dataset

The process of recognition is a complex and dynamic phenomenon that evolves alongside the ever-changing landscape of the electronic and digital realm. Despite facing obstacles related to cost, time, and precision, the organization effectively established dominance in the required market and devised optimal devices to facilitate efficient recognition. The Multispectral Palmprint Image Database, upheld by the Chinese Academy of Sciences (CASIA), is the subject of inquiry. CASIA is a comprehensive database dedicated to multispectral recognition, which includes the acquisition of palm vein images as well as the advancement of numerous biometric modalities [35]. This database encompasses a large collection of palm vein images, employing optical and spectral devices to capture the images with utmost precision. It consists of 7,200 high-resolution jpg images of palms, both right and left, obtained from a sample of 100 individuals. Each image has dimensions of 768×576 and is captured using custom-designed multiple spectral imaging devices as detailed in the description. The photos of each hand in this collection are gathered during two distinct sessions. The duration between two sessions exceeds one month. Three samples are presented during each session. Six palm photographs were captured concurrently using six distinct electromagnetic spectrums for each sample. In addition to

white light, the illumination emanates light at wavelengths of 460, 630, 700, 850, and 940 nanometers. Fig. 3 shows that device that used in dataset an example of palm [36].

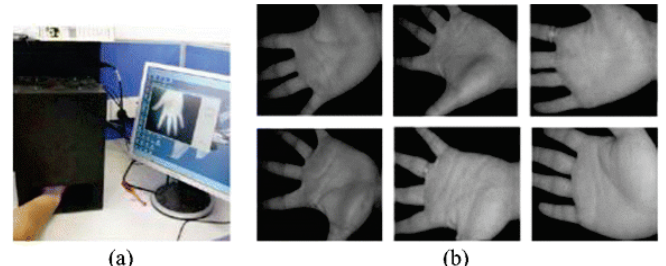


Figure 3 (a) Palmprint Image Scan of "CASIA-Palmprint" dataset in the capture system (b) Some examples of the palmprints [36].

However, the objective of this variety in duration, postures, and light frequency is to attain a state of diversity. The CCD camera is configured to autonomously capture six images of each hand placed in front of a uniformly colored backdrop, without placing any restrictions on the user of the palm vein identification system [37, 36]. Tab. 2 shows the CASIA dataset [38].

Table 2 CASIA multispectral palm print image dataset

Palm number	7200
Sample number	6
Wavelength or light	940 nm, 850 nm, 700 nm, 630 nm, 460 nm and white
Camera type	CCD camera
Image size (pixel)	768×576
Example	

3.2 Pre-processing

Image resizing refers to changing an image's dimensions, making it larger or smaller without cutting off any part of it. In the proposed system, the work was based on changing the size to 256×256 in proportion to the model used. That is, the measurement for this process was done according to experience and which size was the most efficient due to training. The following steps were ROI, which is the context of the palmprint image and stands for the region of interest. The term refers to the precise image region with the most critical palm print identification or examination data. This region typically encompasses the salient characteristics of the palm, such as:

- Palm lines refer to the primary lines on the palm, including the life, heart, and fate lines.
- Palm edges refer to elaborate designs created by elevated and indented skin regions.

- Palm landmarks refer to distinct points of reference on the palm, including the finger base, the palm's midpoint, and the wrist.

The following Fig. 4 shows the steps of resizing and ROI.

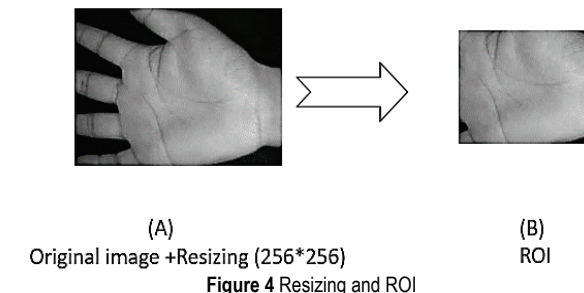


Figure 4 Resizing and ROI

The proposed system implements the CLAHE (Contrast Limited Adaptive Histogram Equalization) as the primary method for adjusting image luminance and enhancing contrast. It effectively addresses issues related to variations in illumination and prevents excessive optimization, which can occur with the conventional histogram equalization [39]. The proposed system initially utilized this technique to enhance low-contrast medical photographs. In contrast to processing the entire image, the CLAHE algorithm operates on squares, which are localized regions of the image. Contrast enhancement utilizes contrast-limited adaptive histogram equalization (CLAHE), a particular application of the histogram equalization method [40] that exhibits adaptive behavior in enhancing the image. The rank of the pixel's intensity in the local intensity histogram is directly proportional to the value by which the pixel's intensity is converted to a value that falls within the display range. CLAHE is an enhanced iteration of Adaptive Histogram Equalization (AHE) that modifies the enhancement procedure through the application of a clip level, which is a user-defined maximum. This clip level restricts the height of the local histogram and, as a result, the maximum contrast enhancement factor. The enhancement is consequently diminished in very homogeneous regions of the image, so preventing excessive amplification of noise and reducing the undesired edge-shadowing effect caused by unrestricted AHE. The CLAHE technique was first devised for medical imaging to mitigate the noise and edge shadowing phenomenon that occurs in uniform regions. The proposed approach applies the Contrast Limited Adaptive Histogram Equalization (CLAHE) algorithm to squares, which are localized regions of the image, rather than the entire image. In this approach, the histogram of each region is calculated as an initial phase. Next, the clipping threshold value is determined based on the required width of the contrast window. In the subsequent stage, every histogram value is reallocated while ensuring it does not exceed the pre-established threshold value. The grayscale mapping process involves determining the Cumulative Distribution Function (CDF) of the histograms in the last stage. The CLAHE approach employs pixel mapping using their immediate four

neighbors. The lower sections are combined using bi-linear interpolation. The regions are categorized into three types, namely IR (interior Region), CR (corner region), and BR (border region), based on their adjacent conditions. Fig. 5 illustrates the sequential resizing process performed prior to applying the ROI and subsequent inclusion of the CLAHE contrast enhancer.

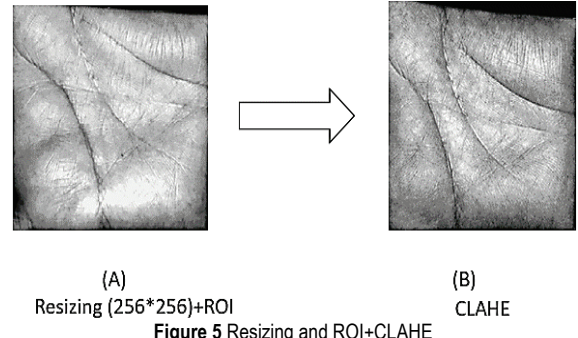


Figure 5 Resizing and ROI+CLAHE

The final step in the proposed system is normalization by using (min-max) in rate (0-1) to measure the standardization of the value of the image. This method scales the un-normalized data to predefined lower and upper bounds. The equation is given as follows:

$$v = \frac{v - \min(A)}{\max(A) - \min(A)} \cdot (\text{newmax}(A) - \text{newmin}(A) + \text{newmin}(A)). \quad (1)$$

The attribute data, represented as A , is defined by its lowest value ($\min(A)$) and maximum value ($\max(A)$). The variable v denotes the revised value for each individual element in the dataset. v denotes the preceding value of every element in the dataset. $\text{newmax}(A)$ refers to the maximum value within the range, while $\text{newmin}(A)$ represents the minimum value within the range (i.e., the boundary values necessary).

3.3 Split Dataset

Hold out technical methods used in the proposed system for split dataset to three sets (training, testing and validation) in a proposed system using (80 % training and 20 % testing). In the Tab. 3 show the division of proportions for training, testing and validation from data set in the proposed system, Fig. 6 illustrates the percentage of each part.

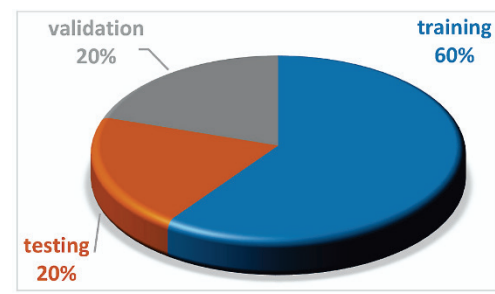


Figure 6 Splitting dataset

Table 3 The percentage of splitting dataset in the proposed system

Training	60 % = 4320
Testing	20 % = 1440
Validation	20 % = 1440

Table 4 Summarizes the layer of dense net 121 in the proposed system

Layer Type	Number of Layers	Function
Conv2D	1	Perform a 7×7 convolution operation with 64 filters, using a stride of 2. Then, apply batch normalization and ReLU activation.
Max Pooling	1	3×3 max pooling with stride 2
Dense Block 1	6	Each layer consists of: * 1×1 convolution with four growth rate filters * 3×3 convolution with growth rate filters * Batch normalization and ReLU activation * Concatenation with all preceding layers in the block.
Transition	1	1×1 convolution with 32 filters, followed by 2×2 average pooling
Dense Block 2	12	Similar to Dense Block 1, but with 32 filters in the 1×1 convolution
Transition	1	1×1 convolution with 64 filters, followed by 2×2 average pooling
Dense Block 3	24	Similar to Dense Block 2, but with 64 filters in the 1×1 convolution
Transition	1	1×1 convolution with 128 filters, followed by 2×2 average pooling
Dense Block 4	16	Similar to Dense Block 3, but with 128 filters in the 1×1 convolution
Global Average Pooling	1	Averages the output of the last Dense block over all spatial dimensions
Dense	1	Fully-connected layer with 1000 neurons (for ImageNet classification)
Softmax	1	Outputs the probability of each class

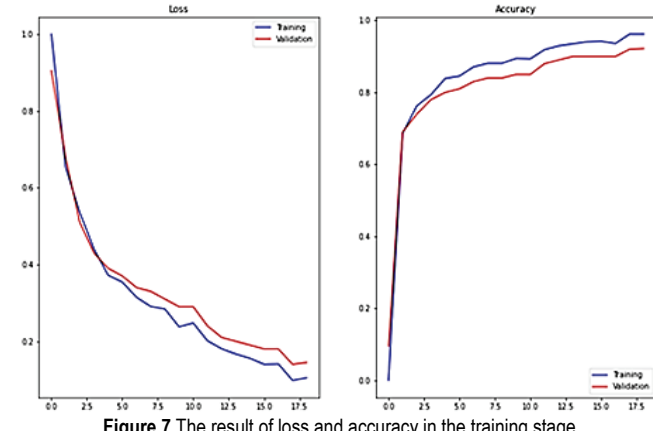
3.4 Training in the Proposed System

DenseNet-121 is a convolutional neural network architecture created in 2017 by Gao Huang and his colleagues. The design is characterized by its dense interconnections between layers, which enhance feature reuse and accuracy compared to other architectures such as VGG and ResNet. Here is a comprehensive analysis of its primary characteristics:

- **Dense Connections:** Unlike conventional CNNs, where each layer only gets input from the previous layer, DenseNet-121 establishes connections between each layer and all prior layers. This facilitates the integration of previously acquired properties into the network, hence improving the transmission of information and the dissemination of distinctive characteristics.
- **DenseNet-121** incorporates bottleneck layers composed of 1×1 and 3×3 convolutional layers. These layers decrease computational complexity and ensure efficient memory usage, all while retaining the ability to extract features effectively.
- **Growth Rate:** The overall output of a Dense Net block is increased by a specific number of feature maps for each layer. The growth rate of the model determines the balance between its complexity and accuracy. The growth rate 12 is utilized in DenseNet-121, which is why it is named as such.

DenseNet-121 incorporates transition layers between Dense blocks to regulate the feature map's size and avoid excessive memory consumption. These layers utilize 1×1 convolutional filters to decrease the number of feature maps and conduct down sampling, resulting in a more condensed and efficient network. The following Tab. 4 shows the layer used in the training stage.

The following Fig. 7 illustrates the result of training in the proposed system.

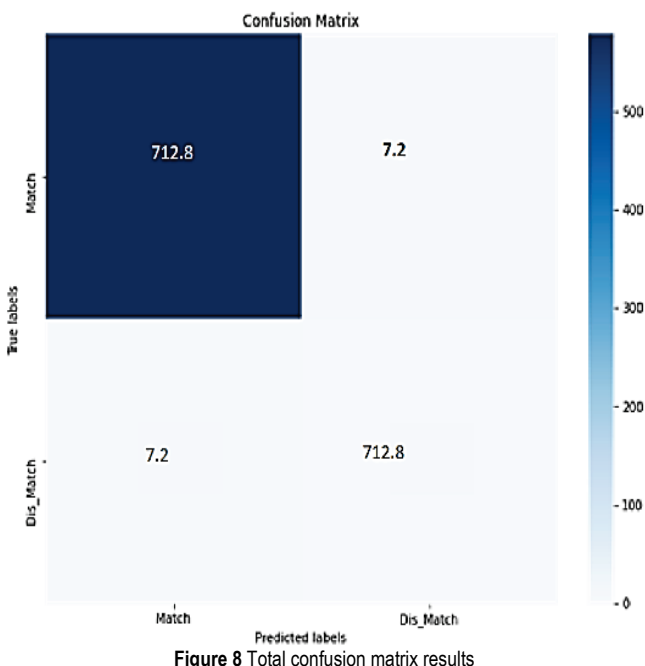
**Figure 7** The result of loss and accuracy in the training stage

3.5 Evaluation of the Proposed System

A confusion matrix is a tabular representation where the rows correspond to the actual subjects and the columns reflect the predicted subjects. A line's presence indicates the quantity of matches. If the row corresponds to the column, meaning that the anticipated value equals the actual value, a mark or dot will be placed [4]. In the absence of such a result, a point will be appended beyond the boundary, signifying the presence of a diagonal line under conditions of high precision. The line signifies the true positive (*TP*) values, which occur when the predicted and actual values coincide ($i = j$). False positive (*FP*) values are denoted by any point above the line ($i \geq j$), while false negative (*FN*) values are represented by any point below the line ($i \leq j$).

The findings were obtained for each true positive (*TP*), false positive (*FP*), false negative (*FN*), and true negative (*TN*) in the confusion matrix for many subjects. The totals for each row and column were extracted and displayed in Fig. 8.

Understanding the calculation process in the deployed system yields eight outputs. The result is this: "The metrics used to evaluate the performance of a classification model are True Positives (*TP*), False Positives (*FP*), True Negatives (*TN*), False Negatives (*FN*), Precision, Recall, F1 score, and accuracy." The scales employed in the system are detailed in Tab. 5. Applicable to the fusion system, the scales' corresponding results are presented alongside an explanation of the measurements.

**Figure 8** Total confusion matrix results**Table 5** Summarizes the result of testing in the proposed system

$TP = 712.8$	$FP = 7.2$	$TN = 712.8$	$FN = 7.2$
Precession		0.99 %	
F1		0.97 %	
Recall		0.98 %	

Table 6 Performance comparison through identification time for CASIA database

Arthur / Reference	Year	Methods	Accuracy
Lian Wu et al. [30]	2021	• Triple-Type Feature Descriptors (TFD) method for Triple-Type Feature Extraction (Texture, Gradient, Direction) then Feature Matching Fusion	88 %
Fatima A Ameen et al. [31]	2022	• VGG16 network, • Features extracted classified using the SoftMax function.	97.32 %
Amjad Rehman et al. [32]	2022	• Return Of Investment (ROI) • MRELBP • k - nearest neighbor classifier.	96.6 %
Mohamed Ezz et al. [41]	2023	• Siamese network • VGG-16	91.8 % on the left images 91.7 % on the right side of dataset
Ebtessam N. AlShemmary et al. [33]	2023	• CNNs	95.6 %
Eslam Hamouda et al. [34]	2023	• HAMTE • Siamese network	90.2 %
Proposed System			

Tab. 6 shows a comparison between research in previous works and what was achieved by the proposed system, what methods were used in previous works, and the accuracy that was achieved.

4 CONCLUSION

Identifying the nature of the palm is one of the topics that has become important in biometric systems because it possesses unique features that cannot be replicated among humans. In the research paper, an approach based on deep learning is proposed using the DenseNet-121 model and through pre-processing of the image by using the CLAHE filter and the normalization process, where the filter had an impact on the accuracy of the results because it worked to clarify the images by working to lighten the areas. Dark areas and blurring the light areas, where he worked on balancing the images of the palm print in the data set CASIA and the normalization process in order to avoid the model entering into a state of overfitting. Standardization of the data was performed and the results obtained were good, with accuracy reaching 99%, precession 0.99, f1 0.97 and recall 0.98.

5 REFERENCES

- [1] Zhong, D., Du, X. & Zhong, K. (2019). Decade progress of palmprint recognition: A brief survey. *Neurocomputing*, 328, 16-28. <https://doi.org/10.1016/j.neucom.2018.03.081>
- [2] Zhang, D., Zuo, W. & Yue, F. (2012). A comparative study of palmprint recognition algorithms. *ACM Comput. Surv.*, 44(1), 1-37. <https://doi.org/10.1145/2071389.2071391>
- [3] Haider AbdAlkreem, M., Sadoon Salman, R. & Khiled Al-Jibory, F. (2024). Detect People's Faces and Protect Them by Providing High Privacy Based on Deep Learning. *Tehnički glasnik*, 18(1), 92-99. <https://doi.org/10.31803/tg-20231210183347>
- [4] Al-Tamimi, M. & AL-Khafaji, R. (2022). Finger vein recognition based on PCA and fusion convolutional neural network. *International Journal of Nonlinear Analysis and Applications*, 13(1), 3667-3681. <https://doi.org/10.22075/ijnaa.2022.6145>
- [5] Genovese, A., Piuri, V. & Scotti, F. (2014). *Touchless palmprint recognition systems*, vol. 60. Springer. <https://doi.org/10.1007/978-3-319-10365-5>
- [6] Al-Taie, S. A. M. & Khaleel, B. I. (2023). Palm Print Recognition Using Intelligent Techniques: A review. *J. Ilm. Tek. Elektro Komput. dan Inform.*, 9(1), 156-164.
- [7] Hamidi, A., Khemgani, S. & Bensid, K. (2021). Transfer learning using vgg based on deep convolutional neural network for finger-knuckle-print recognition. In *Proceedings of the 2nd International Conference on Computer Science's Complex Systems and their Applications*, Oum El Bouaghi, Algeria, pp. 25-26.
- [8] Brown D. & Bradshaw, K. (2019). Improved palmprint segmentation for robust identification and verification. *The 15th IEEE International Conference on Signal-Image Technology & Internet-Based Systems (SITIS2019)*, 1-7. <https://doi.org/10.1109/SITIS2019.00013>
- [9] Li, Q., Dong, P. & Zheng, J. (2020). Enhancing the security of pattern unlock with surface EMG-based biometrics. *Appl. Sci.*, 10(2), p. 541. <https://doi.org/10.3390/app10020541>
- [10] Meena, G. & Choudhary, S. (2019). Biometric authentication in internet of things: A conceptual view. *J. Stat. Manag. Syst.*, 22(4), 643-652. <https://doi.org/10.1080/09720510.2019.1609722>
- [11] Aboot, Q. K. (2023). Predicting Age and Gender Using AlexNet. *TEM J.*, 12(1). <https://doi.org/10.18421/TEM121-61>
- [12] Fei, L., Zhang, B., Xu, Y., Guo, Z., Wen, J. & Jia, W. (2019). Learning discriminant direction binary palmprint descriptor. *IEEE Trans. Image Process.*, 28(8), 3808-3820. <https://doi.org/10.1109/TIP.2019.2903307>

- [13] Rida, I., Al-Maadeed, N., Al-Maadeed, S. & Bakshi, S. (2020). A comprehensive overview of feature representation for biometric recognition. *Multimed. Tools Appl.*, 79, 4867-4890. <https://doi.org/10.1007/s11042-018-6808-5>
- [14] Khaled, F. & Al-Tamimi, M. S. H. (2021). Plagiarism detection methods and tools: An overview. *Iraqi J. Sci.*, 2771-2783. <https://doi.org/10.24996/ijss.2021.62.8.30>
- [15] Miura, N., Nagasaka, A. & Miyatake, T. (2007). Extraction of finger-vein patterns using maximum curvature points in image profiles. *IEICE Trans. Inf. Syst.*, 90(8), 1185-1194. <https://doi.org/10.1093/ietisy/e90-d.8.1185>
- [16] Fei, L., Zhang, B., Tian, C., Teng, S. & Wen, J. (2021). Jointly learning multi-instance hand-based biometric descriptor. *Inf. Sci. (Ny.)*, 562, 1-12. <https://doi.org/10.1016/j.ins.2021.01.086>
- [17] Younis, M. A. & Al-Tamimi, M. S. H. (2022). Preparing of ECG Dataset for Biometric ID Identification with Creative Techniques. *TEM J.*, 11(4).
- [18] Raut, S. D. & Humbe, V. T. (2014). Review of biometrics: palm vein recognition system. *IBMRD's J. Manag. Res.*, 3(1), 217-223.
- [19] Jain, A. K., Ross, A. & Prabhakar, S. (2004). An introduction to biometric recognition. *IEEE Trans. circuits Syst. video Technol.*, 14(1), 4-20. <https://doi.org/10.1109/TCSVT.2003.818349>
- [20] Ungureanu, A.-S., Salahuddin, S. & Corcoran, P. (2020). Toward unconstrained palmprint recognition on consumer devices: A literature review. *IEEE Access*, 8, 86130-86148. <https://doi.org/10.1109/ACCESS.2020.2992219>
- [21] Genovese, A., Piuri, V., Scotti, F. & Vishwakarma, S. (2019). Touchless palmprint and finger texture recognition: A deep learning fusion approach. In *The IEEE International Conference on Computational Intelligence and Virtual Environments for Measurement Systems and Applications (CIVEMSA2019)*, 1-6. <https://doi.org/10.1109/CIVEMSA45640.2019.9071620>
- [22] Meraoumia, A., Chitroub, S. & Bouridane, A. (2011). Fusion of finger-knuckle-print and palmprint for an efficient multi-biometric system of person recognition. In *The IEEE International Conference on Communications (ICC2011)*, 1-5. <https://doi.org/10.1109/icc.2011.5962661>
- [23] Matkowski, W. M., Chan, F. K. S. & Kong, A. W. K. (2019). A study on wrist identification for forensic investigation. *Image Vis. Comput.*, 88, 96-112. <https://doi.org/10.1016/j.imavis.2019.05.005>
- [24] Ungureanu, A.-S., Thavalengal, S., Cognard, T. E., Costache, C. & Corcoran, P. (2017). Unconstrained palmprint as a smartphone biometric. *IEEE Trans. Consum. Electron.*, 63(3), 334-342. <https://doi.org/10.1109/TCE.2017.014994>
- [25] Meitram, R. & Choudhary, P. (2018). Palm vein recognition based on 2D Gabor filter and artificial neural network. *J. Adv. Inf. Technol.*, 9(3). <https://doi.org/10.12720/jait.9.3.68-72>
- [26] Al-Juboori, R. A. L. (2017). Contrast enhancement of the mammographic image using retinex with CLAHE methods. *Iraqi J. Sci.*, 327-336.
- [27] Toygar, Ö., Babalola, F. O. & Bitirim, Y. (2020). FYO: a novel multimodal vein database with palmar, dorsal and wrist biometrics. *IEEE Access*, 8, 82461-82470. <https://doi.org/10.1109/ACCESS.2020.2991475>
- [28] Al-Khafaji, R. S. S. & Al-Tamimi, M. S. H. (2022). Vein Biometric Recognition Methods and Systems: A Review. *Adv. Sci. Technol. Res. J.*, 16(1), 36-46. <https://doi.org/10.12913/22998624/144495>
- [29] Ma, X., Jing, X., Huang, H., Cui, Y. & Mu, J. (2017). Palm vein recognition scheme based on an adaptive Gabor filter. *Iet Biometrics*, 6(5), 325-333. <https://doi.org/10.1049/iet-bmt.2016.0085>
- [30] Wu, L., Xu, Y., Cui, Z., Zuo, Y., Zhao, S. & Fei, L. (2021). Triple-type feature extraction for palmprint recognition. *Sensors*, 21(14), p. 4896. <https://doi.org/10.3390/s21144896>
- [31] Ameen, F. A. & AlShemmary, E. N. (2022). Palmprint Recognition Using VGG16. *Int. J. Tech. Phys. Probl. Eng. IJTPEJournal*, 14(53), 65-74.
- [32] Rehman, A., Harouni, M., Karchegani, N. H. S., Saba, T., Bahaj, S. A. & Roy, S. (2022). Identity verification using palm print microscopic images based on median robust extended local binary pattern features and k-nearest neighbor classifier. *Microsc. Res. Tech.*, 85(4), 1224-1237. <https://doi.org/10.1002/jemt.23989>
- [33] AlShemmary, E. & Ameen, F. A. (2023). Siamese Network-Based Palm Print Recognition. *J. Kufa Math. Comput.*, 10(1), 108-118. <https://doi.org/10.31642/JoKMC/2018/100116>
- [34] Hamouda, E., Ezz, M. M., Mostafa, A. M., Elbashir, M. K., Alruily, M. & Tarek, M. (2023). Innovative Hetero-Associative Memory Encoder (HAMTE) for Palmprint Template Protection. *Comput. Syst. Sci. Eng.*, 46(1), 619-636. <https://doi.org/10.32604/csse.2023.035830>
- [35] Hao, Y., Sun, Z., Tan, T. & Ren, C. (2008). Multispectral palm image fusion for accurate contact-free palmprint recognition. In *The 15th IEEE International Conference on Image Processing*, 281-284.
- [36] Trabelsi, S., Samai, D., Dornaika, F., Benlamoudi, A., Bensid, K. & Taleb-Ahmed, A. (2022). Efficient palmprint biometric identification systems using deep learning and feature selection methods. *Neural Computing and Applications*, 34(14), 12119-12141. <https://doi.org/10.1007/s00521-022-07098-4>
- [37] Datwase, S. S., Deshmukh, R. R. & Gupta, R. S. (2022). Modern Available Palmprint Databases: A Review. *Izvestiya Yuzhnogo federal'nogo universiteta. Tekhnicheskiye nauki*, 3(227), 27-37. <https://doi.org/10.18522/2311-3103-2022-3-27-37>
- [38] Al-Jaberi, A. S. & Al-Juboori, A. M. (2020). Palm vein recognition, a review on prospects and challenges based on CASIA's dataset. In *The 13th IEEE International Conference on Developments in eSystems Engineering (DeSE2020)*, 169-176. <https://doi.org/10.1109/DeSE51703.2020.9450241>
- [39] Zuiderveld, K. (1994). *Graphics Gems IV*. Academic Press, San Diego, CA.
- [40] Kim, J.-W., Kim, S.-B., Park, J.-C. & Nam, J.-W. (2015). Development of crack detection system with unmanned aerial vehicles and digital image processing. *Adv. Struct. Eng. Mech.*, 33(3), 25-29.
- [41] Ezz, M., Alanazi, W., Mostafa, A. M., Hamouda, E., Elbashir, M. K. & Alruily, M. (2023). Improved Siamese Palmprint Authentication Using Pre-Trained VGG16-Palmprint and Element-Wise Absolute Difference. *Comput. Syst. Sci. Eng.*, 46(2). <https://doi.org/10.32604/csse.2023.036567>

Authors' contacts:**Ruu Sadoon Salman**

Ministry of Education, Karkh Three Directorate of Education,
Baghdad, Iraq
ruaa.s.alkhafaji@gmail.com

Mauj Haider AbdAlkreem

(Corresponding author)
Ministry of Education/Administrative Affairs,
Baghdad, Iraq
maujhader7@gmail.com

Qaswaa Khaled Abood

University of Baghdad, College of Science-Computer Science Department,
Baghdad Governorate, Baghdad, Iraq
qaswaa.k@sc.uobaghdad.edu.iq